Eur. Phys. J. C (2024) 84:985
https://doi.org/10.1140/epjc/s10052-024-13366-5

THE EUROPEAN PHYSICAL JOURNAL C

Regular Article - Theoretical Physics

$X_0(2900)$ and its spin partners productions in the B^+ decay processes

Zhuo Yu[1], **Qi Wu**[2], **Dian-Yong Chen**[1,3,a]

[1] School of Physics, Southeast University, Nanjing 210094, China
[2] Institute of Particle and Nuclear Physics, Henan Normal University, Xinxiang 453007, China
[3] Lanzhou Center for Theoretical Physics, Lanzhou University, Lanzhou 730000, China

Received: 12 July 2024 / Accepted: 12 September 2024

Abstract In the present work, we investigate the productions of $X_0(2900)$ and its spin partners in the B^+ decay processes, where $X_0(2900)$ is regarded as a $\bar{D}^*K^*$ molecular state. We infer that the initial B^+ meson and the final $D^+X_0(2900)$ are connected through the $D_{s1}^{\prime+}(2460)\bar{D}^{*0}$ mesons by exchanging a K^{*0} meson. The contributions of such a meson loop to the process $B^+ \to D^+X_0(2900)$ are evaluated and our estimations indicate that the measured branching fraction of $B^+ \to D^+X_0(2900)$ could be well reproduced in a reasonable range of model parameters, indicating that $X_0(2900)$ could be interpreted as a $\bar{D}^*K^*$ molecular state. In addition, the production processes $B^+ \to D^+\tilde{X}_{1,2}$, $B^+ \to D^{*+}X_0(2900)$, and $B^+ \to D^{*+}\tilde{X}_{1,2}$ are investigated, and we find that the fit fraction of $\tilde{X}_1$ in the process $B^+ \to D^{*+}D^{*-}K^+$ is about 6%, which should be accessible by the LHCb and Belle II Collaborations.

1 Introduction

Over the past two decades, there are a growing number of new hadron states reported by the Belle, BESIII, and LHCb collaborations (for further details, refer to the reviews [1–8]). Among these exotic candidates, the majority have been observed in hidden charm channels, exemplified by $X(3872)$ [9] and $Z_c(3900)/Z_c(4020)$ [10,11], which are referred to as the charmonium-like state.

In addition to charmonium-like states, another intriguing category of new hadron states is the fully open flavor states. As typical examples of this kind of new hadron states, $X_{0,1}(2900)$ were observed by the LHCb Collaboration in the D^-K^+ invariant mass distributions of the decay process $B^+ \to D^+D^-K^+$ in 2020 [12,13]. The helicity amplitude analysis indicated that the spins of these two structures were 0 and 1, respectively. Consequently, the J^P quantum numbers of $X_0(2900)$ and $X_1(2900)$ are 0^+ and 1^-, respectively. The measured mass and width of $X_0(2900)$ were,

$$\begin{aligned} m_0 &= (2866 \pm 7 \pm 2)\,\text{MeV}, \\ \Gamma_0 &= (57 \pm 12 \pm 4)\,\text{MeV}, \end{aligned} \tag{1}$$

respectively, while the ones of $X_1(2900)$ were reported to be,

$$\begin{aligned} m_1 &= (2904 \pm 5 \pm 1)\,\text{MeV}, \\ \Gamma_1 &= (110 \pm 11 \pm 4)\,\text{MeV}. \end{aligned} \tag{2}$$

From the observed channel of $X_{0,1}(2900)$, it is apparent that the quark compositions of $X_{0,1}(2900)$ are $ud\bar{s}\bar{c}$, indicating that $X_{0,1}(2900)$ are fully open flavor exotic states. Consequently, investigations into their properties hold significant potential for enhancing our understanding of the non-perturbative behaviors of the strong interaction in QCD. Inspired by the observations of $X_{0,1}(2900)$, various tetraquark interpretations have been proposed in different frameworks. Estimations within the framework of the improved chromo-magnetic interaction model indicated that $X_0(2900)$ could be a compact tetraquark state composed of $ud\bar{s}\bar{c}$ [14]. The masses of the diquark-antidiquark states were estimated by using the QCD sum rule, and the authors in Refs. [15,16] found that $X_0(2900)$ could be assigned as an axialvector-diquark-axialvector-antidiquark type tetraquark state. By considering the SU(3) flavor symmetry, the authors in Ref. [17] interpreted $X_0(2900)$ as the radial excited tetraquark state with $J^P = 0^+$. In Ref. [18], the compact $c\bar{c}s\bar{q}q$ tetraquark states have been systematically estimated in the quark model with the Coulomb, the linear confinement, and the hyperfine interaction, and the estimated mass and width of the ground state with $I(J^P) = 1(0^+)$ are consistent with that of $X_0(2900)$. However, some estimations challenge the tetraquark interpretations of $X_0(2900)$. For instance, the

[a] e-mail: chendy@seu.edu.cn (corresponding author)

Published online: 27 September 2024

estimations in the extended relativized quark model indicate that the mass of the ground state of compact $\bar{c}\bar{s}qq$ tetraquark states with $J^P = 0^+$ is approximately 100 MeV below that of $X_0(2900)$ [19]. Additionally, the masses and widths of both the axial vector and the scalar diquark-antidiquark derived by employing the QCD two-point sum rule method are also inconsistent with those of $X_0(2900)$ [20].

Furthermore, the measured masses of $X_{0,1}(2900)$ are close to the threshold of D^*K^*, suggesting that these two states could be good candidates for the molecular states composed of $\bar{D}^*K^*$. Taking into account the J^P quantum numbers of $X_{0,1}(2900)$, one can find that $X_0(2900)$ and $X_1(2900)$ could be a $S-$wave and $P-$wave $\bar{D}^*K^*$ molecular state, respectively. Before the experimental observation of $X_{0,1}(2900)$, the authors in Ref. [21] predicted the existence of a $D^*\bar{K}^*$ molecule with $J^P = 0^+$ within the hidden-gauge formalism. Subsequent to the observation, the $D^*\bar{K}^*$ molecular interpretations have been further discussed by various groups. For example, estimations within the Bethe-Salpeter framework suggested that $X_0(2900)$ could be identified as a $\bar{D}^*K^*$ molecular state with $I(J^P) = 0(0^+)$ [22,23]. Similarly, investigations within the chiral effective field theory also supported the molecular interpretations of $\bar{D}^*K^*$ of $X_0(2900)$, while $X_1(2900)$ was considered as the P-wave excitation of the ground state $X_0(2900)$ [24]. Using QCD sum rule methods, the mass spectroscopy and decay constants of the $\bar{D}^*K^*$ molecular state had been investigated [25–28], indicating that $X_0(2900)$ could be a $\bar{D}^*K^*$ molecule with $J^P = 0^+$, while $X_1(2900)$ could be considered as a P wave $\bar{c}\bar{s}qq$ tetraquark with $J^P = 1^-$ [27]. In Ref. [29], the D^* and $\bar{K}^*$ interaction was explored in the one-boson exchange model, the mass of $X_0(2900)$ could be reproduced, however, $X_1(2900)$ could not be considered as a $\bar{D}^*K^*$ molecular state with $J^P = 1^-$ as the potential of $\bar{D}^*K^*$ is repulsive in the case of a P wave. In addition, by using the effective Lagrangian approach, the authors in Refs. [30,31] estimated the decay width of $X_0(2900)$, which is in agreement with the experimental measurement within the uncertainty of the model. In addition to tetraquark and molecular interpretations, the kinematical cusp effect [32,33], could also provide insights into understanding these states.

Besides the resonance parameters and decay properties, the production processes are also crucial in decoding the nature of $X_0(2900)$, which sparked numerous theoretical predictions using various approaches. For example, the cross sections for $K^+p \to \Sigma_c^{++}X_0(2900)$ [34] and decay widths of $\Lambda_b \to \Sigma_c^{0,(++)}X_{0,1}^{\prime 0,(--)}$ [35] have been investigated, where $X_{0,1}^{\prime 0,(--)}$ with $su\bar{d}\bar{c}$ ($ds\bar{u}\bar{c}$) are the new $X_{0,1}$-like exotic states. On the experimental side, the fit fraction of $X_0(2900)$ in the process $B^+ \to D^+D^-K^+$ is measured to be $(5.6 \pm 1.4 \pm 0.5)\%$. The branching faction

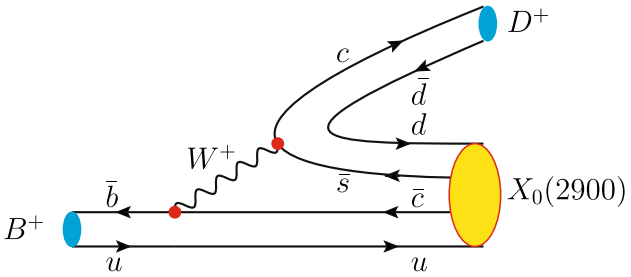

Fig. 1 Diagram contributing to $B^+ \to D^+X_0(2900)$ at the quark level

of $B^+ \to D^+D^-K^+$ is $(2.2 \pm 0.7) \times 10^{-4}$, therefore, the branching fraction of the two-body cascade decay process $B^+ \to D^+X_0(2900) \to D^+(D^-K^+)$ is measured as $(1.2\pm0.5)\times10^{-5}$. The estimations in Refs. [30,31] indicated that $X_0(2900)$ dominantly decays into $\bar{D}K$ channel, where $X_0(2900)$ is considered as a $\bar{D}^*K^*$ molecular state. Considering the isospin symmetry, one can find that the branching fraction of $X_0(2900) \to D^-K^+$ is about 50%, thus one can approximately conclude,

$$\mathcal{B}[B^+ \to D^+X_0(2900)] \approx (2.4 \pm 1.0) \times 10^{-5}. \tag{3}$$

Similar to the process $B^+ \to D^+D^-K^+$, one can also try to search for $X_0(2900)$ in the the process $B^+ \to D^{*+}D^-K^+$. The investigations of the production mechanism of $X_0(2900)$ in the B^+ decay would go a long way towards revealing its nature.

Taking $B^+ \to D^+X_0(2900)$ as an example, we first analyze the process at the quark level, as shown in Fig. 1. The anti-bottom quark transits into an anti-charm quark by emitting a W^+ boson with the up quark as a spectator. Subsequently, the W^+ boson couples to the $c\bar{s}$ quark pair, this weak transition process is phenomenologically described by the operator $\mathcal{H}_W$. Following the creation of $d\bar{d}$ from the vacuum, the c and $\bar{d}$ quark hadronize into a D^+ meson, while the remaining quarks hadronize into $X_0(2900)$. To capture this hadronization process, we employ an operator $\mathcal{H}_T$. Therefore, the process $B^+ \to D^+X_0(2900)$ can be described by the product of $\mathcal{H}_W$ and $\mathcal{H}_T$, denoted as $\mathcal{H} = \mathcal{H}_W\mathcal{H}_T$. Direct estimation of the diagram in Fig. 1 at the quark level is rather difficult. Therefore, in the present work, we simply use the estimations by incorporating a complete basis composed of two mesons. As a result, the decay amplitude becomes

$$\begin{aligned}&\langle D^+X_0(2900)\,|\mathcal{H}|\,B^+\rangle \\ &= \sum_{M_1M_2} \langle D^+X_0(2900)\,|\mathcal{H}_T\,|M_1M_2\rangle\langle M_1M_2|\,\mathcal{H}_W|\,B^+\rangle.\end{aligned} \tag{4}$$

In principle, all the possible $|M_1M_2\rangle$ meson pair that could connect the initial B^+ and final $D^+X_0(2900)$ states should

Table 1 The branching ratios of the relevant processes, where $X_0(2900)$, $\tilde{X}_{1,2}$ may be observed

State	Process	Branching ratio [36]
$X_0(2900)$	$B^+ \to D^+ D^- K^+$	$(2.2 \pm 0.7) \times 10^{-4}$
	$B^+ \to D^{*+} D^- K^+$	$(6.3 \pm 1.1) \times 10^{-3}$
$\tilde{X}_{1,2}$	$B^+ \to D^+ D^{*-} K^+$	$(6.0 \pm 1.3) \times 10^{-4}$
	$B^+ \to D^{*+} D^{*-} K^+$	$(1.32 \pm 0.18) \times 10^{-3}$

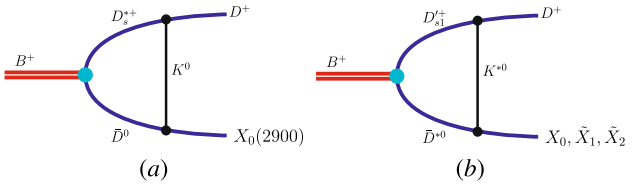

Fig. 2 Diagram contributing to $B^+ \to D^+ X_0(2900)$ and $B^+ \to D^+ \tilde{X}_{1,2}$ at the hadron level. Diagram **a** is the one considered in Ref. [42], while diagram **b** will be considered in the present estimations

be considered. However, in practice, only the dominant contributions are taken into account at the hadron level, which will be discussed in the following section.

Moreover, in the molecular frame, $X_0(2900)$ is regarded as an S-wave $\bar{D}^* K^*$ molecular state. In addition to the 0^+ state, corresponding to $X_0(2900)$, the J^P quantum numbers of the $S-$wave $\bar{D}^* K^*$ system could also be 1^+ and 2^+. In Ref. [37], with the assumption that $X_0(2900)$ is a $I(J^P) = 0(0^+)$ $\bar{D}^* K^*$ hadronic molecule, the potential of $\bar{D}^* K^*$ interactions could be determined and $\bar{D}^* K^*$ molecular states with $I(J^P) = 0(1^+)$ and $I(J^P) = 0(2^+)$ were predicted. Although the estimations in the one-boson exchange model respecting heavy-quark spin symmetry indicated that $X_0(2900)$ could be a $\bar{D}^* K^*$ hadronic molecule with $I(J^P) = 0(0^+)$, and an additional bound state with $I(J^P) = 0(1^+)$ was predicted, while that with $I(J^P) = 0(2^+)$ could be unbounded [29]. Similar conclusions had been drawn in Ref. [38] but the one with $I(J^P) = 0(2^+)$ could be a virtual state. By fine-tuning the model parameters to reproduce exactly the mass and width of $X_0(2900)$ in the local hidden gauge formalism, two more states with $J^P = 1^+$ and 2^+ were reported in Ref. [39], and these two additional states have been proposed to be searched in the processes $\bar{B}^0 \to K^{*0} D^{*+} K^-$ [40] and $B^+ \to D^+ D^- K^+$ [41]. From the above literature, one can conclude that the spin partners of $X_0(2900)$ more likely exist if one considers $X_0(2900)$ as a $\bar{D}^* K^*$ hadronic molecule. Thus, searching for its spin partners should also shed light on the molecular nature of $X_0(2900)$. Hereafter, we use $\tilde{X}_1$ and $\tilde{X}_2$ refer to the spin partners of $X_0(2900)$ with $J^P = 1^+$ and $J^P = 2^+$, respectively.[1] As indicated in Ref. [30], $\tilde{X}_1$ and $\tilde{X}_2$ should predominantly decay into $D^* K$, consequently, one can search for $\tilde{X}_1$ and $\tilde{X}_2$ in processes $B^+ \to D^{(*)+} D^{*-} K^+$. In Table 1, we collected the branching ratios of the relevant processes, where $X_0(2900)$, $\tilde{X}_{1,2}$ may be observed.

This work is organized as follows. After introduction, we present our analysis of the production mechanisms that work in the processes $B^+ \to D^{(*)+} X_0(2900)$, and $B^+ \to D^{(*)+} \tilde{X}_J$, $(J = 1, 2)$, the branching fractions of these processes are estimated in Sect. 2. The numerical results and related discussions are presented in Sect. 3, and the last section is devoted to a short summary.

2 $X_0(2900)$ and its spin partners productions in the B decay process

2.1 Production mechanism at the hadron level

As indicated in Eq. (4), all the allowed meson pairs should be taken into account and in practice, only the dominant contributions are considered at the hadron level. For instance, in Ref. [42], the authors investigate the process $B^+ \to D^+ X_0(2900)$ by assuming the loop in Fig. 2a as the dominant contributions. This choice is based on the observation that the branching fraction of $B^+ \to D_s^{*+} \bar{D}^0$ is $(7.6 \pm 1.6) \times 10^{-3}$, which is approximately two orders of magnitude larger than that of $B^+ \to D^+ X_0(2900)$, and $X_0(2900)$ predominantly decay into $\bar{D}K$ final states.[2] However, in Ref. [42], when the authors estimated the branching fractions of $B^- \to D^- X_0(2900)$ from the fit fraction of $X_0(2900)$, a factor 2 resulting from the branching fractions of $X_0(2900) \to D^+ K^-$ being 50% is missed, and then the obtained branching fraction of $B^+ \to D^- X_0(2900)$ is underestimated with a factor 1/2. In the molecular frame, $X_0(2900)$ is composed of $\bar{D}^*$ and K^*, indicating a strong coupling between $X_0(2900)$ and its components $\bar{D}^* K^*$. Furthermore, the branching fraction of $B^+ \to D_{s1}'(2460)^+ \bar{D}^*$ is measured to be $(1.2 \pm 0.3)\%$, which is approximately three orders of magnitude larger than that of $B^+ \to D^+ X_0(2900)$. Moreover, the charmed-strange meson $D_{s1}'(2460)^+$ couples to $D^+ K^*$ via the S-wave. Thus, we anticipate that the digram depicted in Fig. 2b should play a crucial role in the process $B^+ \to D^+ X_0(2900)$ if $X_0(2900)$ is assigned as a $\bar{D}^* K^*$ molecular state. Similarly, the spin partners of $X_0(2900)$, $\tilde{X}_1$ and $\tilde{X}_2$, could be reproduced with the same mechanism. In addition, if one replaces the final D^+ with D^{*+}, the intermediate states could be both $D_{s1}'(2460)^+$ and $D_{s0}^*(2317)^+$,

[1] It is worth mentioning that the $C-$parity of $X_1(2900)$ observed by the LHCb Collaboration is negative, while the one of the spin partners of $X_0(2900)$ is positive.

[2] In Ref. [42], the authors investigated the process $B^- \to D^- \bar{X}_0(2900)$. The mechanism operating in $B^- \to D^- \bar{X}_0(2900)$ should be the same as in $B^+ \to D^+ X_0(2900)$.

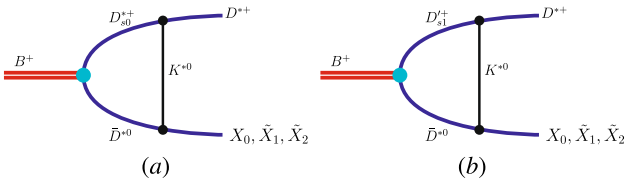

Fig. 3 Diagram contributing to $B^+ \to D^{*+}X_0, \tilde{X}_{1,2}$ at the hadron level

since both states couple to $D^{*+}K^{*0}$ via the S wave. The diagrams contributing to $B^+ \to D^{*+}X_0, \tilde{X}_{1,2}$ are presented in Fig. 3.

In our current study, we evaluate the contributions of Fig. 2b to $B^+ \to D^+X_0(2900)$ and compare our estimations with the experimental data in Eq. (3), and this comparison could be a crucial test for the $\bar{D}^*K^*$ molecular interpretations to $X_0(2900)$. In addition, with the parameter range determined by the process $B^+ \to D^+X_0(2900)$, we can evaluate the branching fractions of $B^+ \to D^+\tilde{X}_{1,2}$ and $B^+ \to D^{*+}X_0, \tilde{X}_{1,2}$, which may provide some helpful information for searching the spin partners of $X_0(2900)$ in the B^+ decay processes.

2.2 Effective Lagrangian

As discussed above, the contribution of the loop illustrated in Figs. 2b and 3 is expected to be dominant for the process $B^+ \to D^{(*)+}X_0, \tilde{X}_1, \tilde{X}_2$ when considering $X_0(2900)$ as the $\bar{D}^*K^*$ molecular state with $I(J^P) = 0(0^+)$, while $\tilde{X}_1, \tilde{X}_2$ are the spin partners of $X_0(2900)$ with $J = 1$ and $J = 2$, respectively. In this study, all hadron interactions are described by the effective Lagrangian approach. As for the effective Lagrangian for the coupling between X_0 and $\tilde{X}_{1,2}$ with its components, we employ the simple S-wave coupling, which are [30],

$$\begin{aligned}
\mathcal{L}_{X_0D^*K^*} &= g_{X_0}X_0\left[D^{*-\mu}K^{*+}_{\mu} - \bar{D}^{*0\mu}K^{*0}_{\mu}\right],\\
\mathcal{L}_{\tilde{X}_1D^*K^*} &= g_{\tilde{X}_1}\varepsilon_{\mu\nu\alpha\beta}\partial^{\mu}\tilde{X}_1^{\nu}\left[D^{*-\alpha}K^{*+\beta} - \bar{D}^{*0\alpha}K^{*0\beta}\right],\\
\mathcal{L}_{\tilde{X}_2D^*K^*} &= g_{\tilde{X}_2}\tilde{X}_2^{\mu\nu}\left[D^{*-}_{\mu}K^{*+}_{\nu} - \bar{D}^{*0}_{\mu}K^{*0}_{\nu}\right],
\end{aligned} \tag{5}$$

where g_{X_0} and $g_{\tilde{X}_1/\tilde{X}_2}$ are the effective coupling constants, and their values will be discussed later. As for the weak interaction vertex $B^+ \to D'_{s1}(2460)^+/D^*_{s0}(2317)^+\bar{D}^{*0}$, we utilize the parametrized hadronic matrix elements obtained by the effective Hamiltonian at the quark level, which are [43,44],

$$\begin{aligned}
&\langle 0|J_{\mu}|D^*_{s0}(p_1)\rangle = -if_{D^*_{s0}}p_{1\mu},\\
&\langle 0|J_{\mu}|D'_{s1}(p_1,\epsilon)\rangle = f_{D'_{s1}}\epsilon(p_1)_{\mu}m_{D_{s1}},\\
&\langle D^*(p_2,\epsilon)|J_{\mu}|B(p_0)\rangle\\
&= \frac{i\epsilon^{\nu}}{m_B + m_{D^*}}\Big\{i\varepsilon_{\mu\nu\alpha\beta}P^{\alpha}q^{\beta}V(q^2)\\
&-(m_B + m_{D^*})^2\, g_{\mu\nu}A_1(q^2) + P_{\mu}P_{\nu}A_2(q^2)\\
&+2m_{D^*}\,(m_B + m_{D^*})\,\frac{P_{\nu}q_{\mu}}{q^2}\left[A_3(q^2) - A_0(q^2)\right]\Big\},
\end{aligned} \tag{6}$$

with $J_{\mu} = \bar{q}_1\gamma_{\mu}(1-\gamma_5)q_2$, $P_{\mu} = p_{0\mu} + p_{2\mu}$ and $q_{\mu} = p_{0\mu} - p_{2\mu}$. $A_{0,1,2}(q^2)$ and $V(q^2)$ are the weak transition form factors, while $A_3(q^2)$ is the linear combination of form factors $A_1(q^2)$ and $A_2(q^2)$, which is [43],

$$A_3(q^2) = \frac{m_B + m_{D^*}}{2m_{D^*}}A_1(q^2) - \frac{m_B - m_{D^*}}{2m_{D^*}}A_2(q^2). \tag{7}$$

With the above hadronic matrix elements, we can get the amplitude of weak interaction vertex $B^+(p_0) \to D^+_{sJ}(p_1)\bar{D}^*(p_2)$, which are,

$$\begin{aligned}
\mathcal{A}(B^+ \to D'_{s1}\bar{D}^{*0}) &= A^{B^+\to D'^+_{s1}\bar{D}^{*0}}_{\mu\nu}(p_1,p_2)\epsilon^{\mu}_{D'_{s1}}\epsilon^{\nu}_{\bar{D}^*}\\
&= \frac{G_F}{\sqrt{2}}V_{cb}V_{cs}a_1\left\langle D^+_{sJ}\left|J_{\mu}\right|0\right\rangle\left\langle\bar{D}^{*0}\left|J^{\mu}\right|B^+\right\rangle,\\
\mathcal{A}(B^+ \to D^{*+}_{s0}\bar{D}^{*0}) &= A^{B^+\to D^{*+}_{s0}\bar{D}^{*0}}_{\nu}\epsilon^{\nu}_{\bar{D}^*}\\
&= \frac{G_F}{\sqrt{2}}V_{cb}V_{cs}a_1\left\langle D^+_{s0}\left|J_{\mu}\right|0\right\rangle\left\langle\bar{D}^{*0}\left|J^{\mu}\right|B^+\right\rangle,
\end{aligned} \tag{8}$$

where G_F is the Fermi constant, V_{bc} and V_{cs} are the CKM matrix elements. $a_1 = c_1^{eff} + c_2^{eff}/N_c$ with $c_{1,2}^{eff}$ being the effective Wilson coefficients, obtained by the factorization approach [45], and $N_c = 3$ is the number of the color of the quark. In the present work, we adopt $G_F = 1.166 \times 10^{-5}\,\mathrm{GeV}^{-2}$, $V_{cb} = 0.041$, $V_{cs} = 0.987$ and $a_1 = 1.05$, $f_{D'_{s1}} = 158$ MeV, $f_{D^*_{s0}} = 70$ MeV as in Refs. [36,46–48].

For the effective coupling relevant to the charmed mesons, they can be constructed in the heavy-quark limit and chiral symmetry. In the heavy quark limit, the $S-$wave heavy-light mesons can be described by the superfield $H_a^{(Q)}$, which is

$$H_a^{(Q)} = \frac{1+\not{v}}{2}\left[P_a^{*(Q)\mu}\gamma_{\mu} - P_a^{(Q)}\gamma_5\right], \tag{9}$$

where P^* and P refer to the vector and pseudosclar S-wave heavy light mesons, respectively.

For the $P-$wave heavy-light mesons, they are devided into two doublets depending on the light degree of freedom, which are $S-$doublet with $s_{\ell} = 1/2$ and $T-$doublet with $s_{\ell} = 3/2$. The involved $D'^+_{s1}(2460)$ and $D^*_{s0}(2317)^+$ belong to the $S-$doublet, and the concrete form of the $S-$double superfield is,

$$S_a^{(Q)} = \frac{1+\not{v}}{2}\left[P_{1a}^{\prime(Q)\mu}\gamma_{\mu}\gamma_5 - P_{0a}^{*(Q)}\right], \tag{10}$$

with P'_1 and P^*_0 to be $P-$wave heavy light meson in the S-doublet with $J = 1$ and $J = 0$, respectively.

In terms of heavy quark limit and chiral symmetry, the effective Lagrangians has been constructed in the literatures as [49–51],

$$\mathcal{L}_V = i\zeta \left\langle H_b^{(Q)} \gamma^\mu \left(-\rho_\mu\right)_{ba} \bar{S}_a^{(Q)} \right\rangle + i\mu \left\langle H_b^{(Q)} \sigma^{\lambda\nu} F_{\lambda\nu}(\rho)_{ba} \bar{S}_a^{(Q)} \right\rangle + \text{H.c}, \tag{11}$$

where $F_{\mu\nu}(\rho) = \partial_\mu \rho_\nu - \partial_\nu \rho_\mu + [\rho_\mu, \rho_\nu]$, and ρ_μ is defined as

$$\rho_\mu = i \frac{g_V}{\sqrt{2}} \mathcal{V}_\mu. \tag{12}$$

$\mathcal{V}_\mu$ is matrix form of the light vector mesons with the concrete form as,

$$\mathcal{V} = \begin{pmatrix} \frac{\rho^0}{\sqrt{2}} + \frac{\omega}{\sqrt{2}} & \rho^+ & K^{*+} \\ \rho^- & -\frac{\rho^0}{\sqrt{2}} + \frac{\omega}{\sqrt{2}} & K^{*0} \\ K^{*-} & \bar{K}^{*0} & \phi \end{pmatrix}. \tag{13}$$

Since we only focus on the S-wave coupling in the present work, which means the term with constant μ in Eq. (11) should be neglected, so we obtained the detailed Lagrangian of $\mathcal{D}_1' \mathcal{D}^{(*)} \mathcal{V}$ and $\mathcal{D}_0 \mathcal{D}^* \mathcal{V}$, which reads,

$$\begin{aligned} \mathcal{L}_{\mathcal{D}_1' \mathcal{D} \mathcal{V}} &= g_{\mathcal{D}_1' \mathcal{D} \mathcal{V}} \mathcal{D}_{1b}'^{\mu} \mathcal{V}_{\mu_{ba}} \mathcal{D}_a^\dagger \\ \mathcal{L}_{\mathcal{D}_1' \mathcal{D}^* \mathcal{V}} &= i\, g_{\mathcal{D}_1' \mathcal{D}^* \mathcal{V}} \varepsilon_{\mu\nu\alpha\beta} \mathcal{V}_{ba}^{*\nu} \mathcal{D}_b^{*\mu} \overleftrightarrow{\partial^\beta} \mathcal{D}_{1a}'^{\alpha\dagger} \\ \mathcal{L}_{\mathcal{D}_0^* \mathcal{D}^* \mathcal{V}} &= g_{\mathcal{D}_0^* \mathcal{D}^* \mathcal{V}} \mathcal{D}_b^{\mu} \mathcal{V}_{\mu_{ba}} \mathcal{D}_{0a}^{*\dagger} \end{aligned} \tag{14}$$

where the $\mathcal{D}$ is charmed meson triplets (D^0, D^+, D_s^+), while $\mathcal{D}^*$, $\mathcal{D}_1'$, and $\mathcal{D}_0^*$ have the similar definitions. The relevant coupling constants will be discussed later.

2.3 Decay amplitude

With the above effective Lagrangians, the amplitude of $B^+(p_0) \to [D_{s1}'^+(p_1)\bar{D}^{*0}(p_2)]K^{*0}(q) \to D^+(p_3) X_0(2900)(p_4)$ corresponding to Fig. 2b could be obtained as,

$$\begin{aligned} \mathcal{M} = i^3 \int \frac{d^4q}{(2\pi)^4} &\left[\mathcal{A}_{\mu\nu}^{B^+ \to D_{s1}'^+ \bar{D}^{*0}}(p_1, p_2)\right] \left[i g_{D_{s1}' D K^*} g_{\alpha\beta}\right] \left[i g_{X_0} g_{\rho\phi}\right] \\ &\times \left[\frac{-g^{\mu\alpha} + p_1^\mu p_1^\alpha / m_1^2}{p_1^2 - m_1^2}\right] \left[\frac{-g^{\nu\rho} + p_2^\nu p_2^\rho / m_2^2}{p_2^2 - m_2^2}\right] \\ &\times \left[\frac{-g^{\beta\phi} + q^\beta q^\phi / m_q^2}{q^2 - m_q^2}\right] \mathcal{F}^2\left(q^2, m_q^2\right). \end{aligned} \tag{15}$$

where $\mathcal{A}_{\mu\nu}^{B^+ \to D_{s1}'^+ \bar{D}^{*0}}(p_1, p_2)$ is defined in Eq. (8). The rest amplitudes corresponding to Figs. 2b and 3 can be found in the appendix A.

In the above amplitude, we introduce a form factor $\mathcal{F}(q^2, m^2)$ in monopole form to compensate for the off-shell effect and to avoid ultraviolet divergence in the loop integral. Its concrete form is,

$$\mathcal{F}(q^2, m^2) = \frac{m^2 - \Lambda^2}{q^2 - \Lambda^2}, \tag{16}$$

where $\Lambda = m + \alpha \Lambda_{\text{QCD}}$ is the cut-off parameter [52], with $\Lambda_{\text{QCD}} = 220$ MeV and α to be the model parameter. It should be noted that the form factor also plays the role of describing the momentum dependence of the coupling between $X_0(2900)$ and its components as indicated in Ref. [53,54].

Then, the partial width of $B^+ \to D^+ X_0(2900)$ can be obtained by,

$$\Gamma_{B^+ \to D^+ X_0} = \frac{1}{8\pi} \frac{|\vec{p}|}{m_B^2} \overline{|\mathcal{M}_{B^+ \to D^+ X_0}|^2}, \tag{17}$$

and consequently, we can obtain the branching fraction of $B^+ \to D^+ X_0(2900)$ depending on the model parameter α.

3 Numerical results and discussions

3.1 Coupling constants

Before we estimate the branching ratio of $B^+ \to D^{(*)+} X(2900)$, some relevant coupling constants should be further clarified. The coupling constant of $X_0(2900)$, $\tilde{X}_{1,2}$ with their components could be estimated by the compositeness conditions in the molecular frame. In Ref. [30], the authors estimated the decay properties of X_0 and $\tilde{X}_{1,2}$ in the molecular frame and found that the measured width of $X_0(2900)$ could be well reproduced. In the considered range of model parameter, the coupling constants g_{X_0} and $g_{\tilde{X}_{1,2}}$ were estimated to be approximately 9.11 GeV, 3.84 and 16.28 GeV, respectively.

As for the weak transition form factor, the estimations in Refs. [43,44] parametrized them in the form,

$$F(Q^2) = \frac{F(0)}{1 - a\zeta + b\zeta^2} \tag{18}$$

with $\zeta = Q^2/m_B^2$. The relevant parameters $F(0)$, a, and b for each form factor are collected in Table 2. In the present work, we calculate the amplitude by Feynman parameterization method with the help of `FeynCalc` and `LoopTools` packages [55,56], where both absorptive and dispersive parts are included. To simplify the estimations, we further parametrize Eq. (18) in the form,

$$F(Q^2) = F(0) \frac{\Lambda_1^2}{Q^2 - \Lambda_1^2} \frac{\Lambda_2^2}{Q^2 - \Lambda_2^2}. \tag{19}$$

By fitting Eq. (18) with Eq. (19), we can obtain the values of Λ_1 and Λ_2 for each form factor, which are listed in Table 3.

Table 2 The values of the parameters $F(0)$, a and b in the form factors [58]

Parameter	$F(0)$	a	b
A_0	0.68	1.21	0.36
A_1	0.65	0.60	0.00
A_2	0.61	1.12	0.31
V	0.77	1.25	0.38

Table 3 Values of the parameters Λ_1 and Λ_2 obtained by fitting Eq. (18) with Eq. (19)

Parameter	A_0	A_1	A_2	V
Λ_1	6.5	8.95	6.65	6.30
Λ_2	7.1	8.75	7.55	7.10

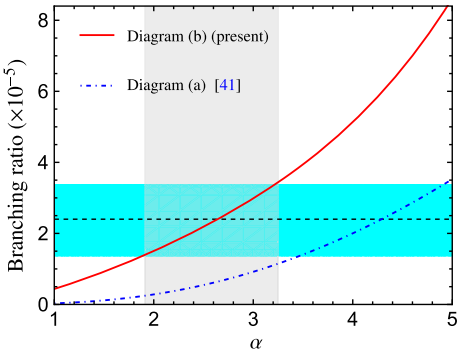

Fig. 4 The α dependences of branching ratios of $B^+ \to X_0(2900)D^+$ (in unit of 10^{-5}) contributing from different diagrams. The horizontal black dashed line with cyan band indicates the measured branching ratios of $B^+ \to X_0(2900)D^+$, while the vertical light grey band refers to the α range in which the measured branching fraction could be reproduced by the contributions from diagram (b)

Considering the heavy quark limit and chiral symmetry, the coupling constants of $\mathcal{D}_{1,0}\mathcal{D}^{(*)}\mathcal{V}$ in Eq. (14) are given as [57],

$$\begin{aligned} g_{\mathcal{D}_1'\mathcal{D}\mathcal{V}} &= -\sqrt{2}\zeta g_V \sqrt{M_{\mathcal{D}_1'} M_{\mathcal{D}}} \\ g_{\mathcal{D}_0^*\mathcal{D}^*\mathcal{V}} &= -\sqrt{2}\zeta g_V \sqrt{M_{\mathcal{D}_0^*} M_{\mathcal{D}^*}} \\ g_{\mathcal{D}_1'\mathcal{D}^*\mathcal{V}} &= \sqrt{2}\zeta g_V, \end{aligned} \tag{20}$$

with $g_V \simeq 5.8$ by imposing the Kawarabayashi–Suzuki–Riazuddin–Fayyazuddin relations [57] and $\zeta = 0.1$ [49].

3.2 Branching fractions

With the above preparations, all relevant coupling constants have been fixed except the model parameter α. This parameter of the phenomenological model cannot be determined by the first principle methods. As indicated in Ref. [52], α should be of order unity. In the present estimation, we vary α from 1 to 5 to check the parameter dependence of the branching fractions. By reproducing the experimental data in Eq. (3), we can determine the value of parameter α and check the rationality of the parameter range, which can further test the $\bar{D}^*K^*$ molecular interpretations to the $X_0(2900)$. In addition, considering the similarity of $X_0(2900)$, $\tilde{X}_1$ and $\tilde{X}_2$, we can evaluate the production ratios of $B^+ \to D^+\tilde{X}_{1,2}$ and $B^+ \to D^{*+}X_0, \tilde{X}_{1,2}$ in the same model parameter range, which should be helpful for experimentally searching for the spin partners of $X_0(2900)$.

The branching ratio of $B^+ \to D^+X_0(2900)$ depending on the model parameter α is presented in Fig. 4. The solid red and dashed blue curves are contributions of diagram (b) and diagram (a), respectively.[3] From the figure, one can find that the branching fraction contributing from both diagrams (a) and (b) increases with increasing model parameter α, and the contribution from diagram (b) is several times larger than that from diagram (a), which is consistent with our expectations discussed in Sect. 2.1. Moreover, from Fig. 4, one can find that the α dependences of the contributions from diagram (a) and (b) are very similar, thus, we can expect that the less important contributions from diagram (a) could be included by the predominant contribution form diagram (b) to a certain extent by adjusting the model parameter α. In addition, in the calculations of the diagram (a), the coupling constant g_{X_0DK} is estimated by the measured width of $X_0(2900)$ with the assumption that $X_0(2900)$ dominately decays into DK. However, when we extend our estimations to predict the production branching fractions of the unobserved spin partners of $X_0(2900)$, the coupling constants for $\tilde{X}_1D^*K/\tilde{X}_1DK^*$ and $\tilde{X}_2DK$ could not be well determined. Thus, in the present work, we only consider the contributions of diagram (b). Here, the experimental measurement from the LHCb Collaboration is also presented for comparison. Our estimation could well reproduce the experimental data in the range $1.9 < \alpha < 3.2$, which is of order unity. Thus, we can conclude that the $\bar{D}^*K^*$ molecular interpretations to the $X_0(2900)$ should be reasonable.

Similarly, we can investigate the process $B^+ \to D^+\tilde{X}_{1,2}$, where $\tilde{X}_1$ and $\tilde{X}_2$ are the spin partners of $X_0(2900)$ with $J = 1$ and $J = 2$, respectively. The branching ratios of $B^+ \to D^+\tilde{X}_{1,2}$ depending on the model parameter α are presented in Fig. 5. Our estimations indicate that these two branching ratios are very close, but one order of magnitude smaller than $B^+ \to D^+X_0(2900)$. In particular, in the parameter range determined by $B^+ \to D^+X_0(2900)$, the branching ratios of $B^+ \to D^+\tilde{X}_{1,2}$ are predicted to be $(0.5 \sim 1.1) \times 10^{-6}$. As indicated in Ref. [30], $\tilde{X}_{1,2}$ predominantly decays into $\bar{D}^*K$, and the branching ratios of $\tilde{X}_{1,2} \to D^{*-}K^+$ are approximately 40%. Thus, we can approximately obtain the

[3] The contributions from diagram (a) is taken from Ref. [42].

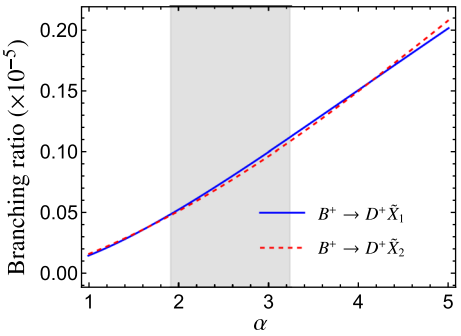

Fig. 5 The branching fraction of $B^+ \to D^+\tilde{X}_{1/2}(2900)$ (in unit of 10^{-5}) depending on the model parameter α. The vertical light grey band refers to the α range determined by $B^+ \to D^+X_0(2900)$

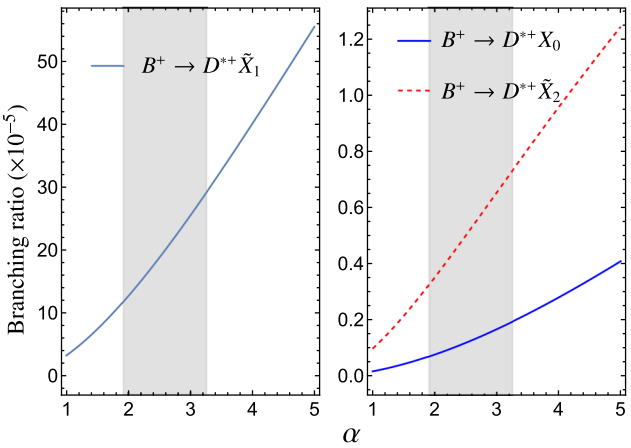

Fig. 6 The branching fractions of $B^+ \to D^{*+}X_0(2900)$, $\tilde{X}_{1,2}$ (in unit of 10^{-5}) depending on the model parameter α. The vertical light grey band refers to the α range determined by $B^+ \to D^+X_0(2900)$

branching fraction of $B^+ \to D^+\tilde{X}_{1,2} \to D^+D^{*-}K^+$ to be of order 10^{-7}, indicating that the fit fractions of $\tilde{X}_{1,2}$ in $B^+ \to D^+D^{*-}K^+$ are of order 10^{-3}. Thus, it is impossible to search the spin partners of $X_0(2900)$ in the process $B^+ \to D^+D^{*-}K^+$.

In addition to $B^+ \to D^+X_0(2900)$, $\tilde{X}_{1,2}$, we also investigate the production process $B^+ \to D^{*+}X_0(2900)$, $\tilde{X}_{1,2}$ in the present work. The branching fractions of the relevant processes depending on the model parameter α are presented in Fig. 6. In the left panel, we present the branching fractions of the process $B^+ \to D^{*+}\tilde{X}_1$. The present estimations indicate that in the parameter range determined by $B^+ \to D^+X_0(2900)$, the branching fraction of $B^+ \to D^{*+}\tilde{X}_1$ is $(1.2 \sim 2.9) \times 10^{-4}$, which is approximately one order of magnetite larger than that of $B^+ \to D^+X_0(2900)$. As listed in Table 1, the branching fraction of $B^+ \to D^{*+}D^{*-}K^+$ is $(1.32 \pm 0.18) \times 10^{-3}$, therefore, the fit fraction of $B^+ \to D^{*+}\tilde{X}_1 \to D^{*+}D^{*-}K^+$ is about 6% with the assumption that the branching fraction of $\tilde{X}_1 \to D^{*-}K^+$ is about 40% [30]. Compared to the fit fraction of $X_0(2900)$ in the process $B^+ \to D^+D^-K^+$ being $(5.6 \pm 1.4 \pm 0.5)\%$, we can conclude that experimentally searching for $\tilde{X}_1$ in the process $B^+ \to D^{*+}D^{*-}K^+$ is possible. The predicted branching fractions of the processes $B^+ \to D^{*+}X_0(2900)$ and $B^+ \to D^{*+}\tilde{X}_2$ are present in the right panel of Fig. 6. In the determined α range, the branching fraction of $B^+ \to D^{*+}X_0(2900)$ is estimated to be $(0.7 \sim 1.9) \times 10^{-6}$, which is at least one order smaller than that of $B^+ \to D^+X_0(2900)$. For $B^+ \to D^{*+}\tilde{X}_2$, the predicted branching fraction is $(3.2 \sim 7.2) \times 10^{-6}$, which is about several times smaller than that of $B^+ \to D^+X_0(2900)$. Considering that the branching fraction of $B^+ \to D^{*+}D^{*-}K^+$ is of the order 10^{-3}, the fit fraction of $\tilde{X}_2$ in $B^+ \to D^{*+}D^{*-}K^+$ is of the order 10^{-3}, which indicates that searching for $X_0(2900)$ in the process $B^+ \to D^{*+}D^-K^+$ and searching for $\tilde{X}_2$ in the process $B^+ \to D^{*+}D^{*-}K^+$ are both impossible. In Table 4, we summarize the predicted branching fractions of the relevant processes and the experimental potential of searching for $X_0(2900)$ and its spin partners in the corresponding processes.

Table 4 Branching ratios of all decay modes considered in the present work. The symbols ✓ and ✗ indicate the experimental potential of searching $X_0(2900)$ and its spin partners in the corresponding processes

Process	Branching ratio	Status
$B^+ \to D^+X_0$	$(1.4 \sim 2.4) \times 10^{-5}$	Input
$B^+ \to D^+\tilde{X}_1$	$(0.5 \sim 1.1) \times 10^{-6}$	✗
$B^+ \to D^+\tilde{X}_2$	$(0.5 \sim 1.1) \times 10^{-6}$	✗
$B^+ \to D^{*+}X_0$	$(0.7 \sim 1.9) \times 10^{-6}$	✗
$B^+ \to D^{*+}\tilde{X}_1$	$(1.2 \sim 2.9) \times 10^{-4}$	✓
$B^+ \to D^{*+}\tilde{X}_2$	$(3.2 \sim 7.2) \times 10^{-6}$	✗

4 Summary

Since the observation of $X_{0,1}(2900)$ by the LHCb collaboration, various interpretations have been proposed to investigate their internal structure. In particular, tetraquark interpretations were proposed inspired by the fully open flavor properties of $X_{0,1}(2900)$. In addition, the observed mass of $X_{0,1}(2900)$ is close to the threshold of $\bar{D}^*K^*$, and the J^P quantum numbers of the S-wave $\bar{D}^*K^*$ molecule could be consistent with those of $X_0(2900)$, thus, the $\bar{D}^*K^*$ molecular interpretation has been proposed for the $X_0(2900)$. The mass spectroscopy and decay behavior of $X_0(2900)$ have been reproduced in the molecular frame. To further test the rationality of molecular interpretation, we investigate the $X_0(2900)$ production process $B^+ \to D^+X_0(2900)$ in the present work.

In the molecular frame, $X_0(2900)$ is composed of $\bar{D}^*$ and K^*, and we also find that the branching fraction of

$B^+ \to D'_{s1}(2460) + \bar{D}^{*0}$ is measured to be of the order of 10^{-2}, which is approximately three orders of magnitude larger than that of $B^+ \to D^+ X_0(2900)$. Furthermore, it should be noted that $D'_{s1}(2460)^+$ couples to D^+K^* through a S-wave interaction. Thus, we can infer that the initial B^+ meson and the final $D^+X_0(2900)$ could be connected through $D'_{s1}(2460)^+\bar{D}^{*0}$ meson pair by exchanging a K^{*0} meson. Similarly, the spin partners of $X_0(2900)$ could be produced in the process $B^+ \to D^+\tilde{X}_{1,2}$. In addition, the productions of $X_0(2900)$ and its spin partners in the processes $B^+ \to D^{*+}X_0(2900)$, $\tilde{X}_{1,2}$ are also investigated in the present work.

Our estimations indicate that the branching fractions of $B^+ \to D^+X_0(2900)$ could be well reproduced in the parameter range $1.9 < \alpha < 3.2$, which indicates that the $\bar{D}^*K^*$ molecular interpretations for the $X_0(2900)$ should be reasonable. In the same parameter range, we find that the branching fractions of the processes $B^+ \to D^+\tilde{X}_{1,2}$, $B^+ \to D^{*+}X_0(2900)$, and $B^+ \to D^{*+}\tilde{X}_2$ are of the order 10^{-6}. While the branching fraction of the process $B^+ \to D^{*+}\tilde{X}_1$ is of the order 10^{-4}, and the fit fraction of $\tilde{X}_1$ in the process $B^+ \to D^{*+}D^{*-}K^+$ is about 6%, which should be accessible by the LHCb and Belle II Collaborations

Acknowledgements The authors would like to thank Dr. Yan-Ke Chen for providing us with their data and Prof. Fu-Sheng Yu for useful discussions. This work is supported by the National Natural Science Foundation of China under Grants 12175037, 12335001, and 12405093.

Data Availability Statement This manuscript has no associated data. [Authors' comment: Data sharing not applicable to this article as no datasets were generated or analyzed during the current study].

Code Availability Statement This manuscript has no associated code/software. [Authors' comment: There is no code associated in the article].

Funded by SCOAP[3].

Appendix A Decay amplitudes

The amplitudes corresponding the diagrams in Figs. 2 and 3 read,

$$\mathcal{M}_{B^+\to D^+\tilde{X}_1} = i^3 \int \frac{d^4q}{(2\pi)^4}\Big[\mathcal{A}^{B\to D_{s1}\bar{D}^*}_{\mu\nu}(p_1,p_2)\Big] \times \Big[ig_{D_1DV}g_{\alpha\beta}\Big]\Big[-g_{\tilde{X}_1}\varepsilon_{\mu_1\tau\rho\phi}p_4^{\mu_1}\epsilon^{\tau}(p_4)\Big] \times \left[\frac{-g^{\mu\alpha}+p_1^{\mu}p_1^{\alpha}/m_1^2}{p_1^2-m_1^2}\right]\left[\frac{-g^{\nu\rho}+p_2^{\nu}p_2^{\rho}/m_2^2}{p_2^2-m_2^2}\right] \times \left[\frac{-g^{\beta\phi}+q^{\beta}q^{\phi}/m_q^2}{q^2-m_q^2}\right]\mathcal{F}^2\left(q^2,m_q^2\right),$$

$$\mathcal{M}_{B^+\to D^+\tilde{X}_2} = i^3 \int \frac{d^4q}{(2\pi)^4} \times\Big[\mathcal{A}^{B\to D_{s1}\bar{D}^*}_{\mu\nu}(p_1,p_2)\Big]\Big[ig_{D_1DV}g_{\alpha\beta}\Big] \times\Big[ig_{\tilde{X}_2}\epsilon_{\rho\phi}(p_4)\Big]\times\left[\frac{-g^{\mu\alpha}+p_1^{\mu}p_1^{\alpha}/m_1^2}{p_1^2-m_1^2}\right] \times\left[\frac{-g^{\nu\rho}+p_2^{\nu}p_2^{\rho}/m_2^2}{p_2^2-m_2^2}\right]\left[\frac{-g^{\beta\phi}+q^{\beta}q^{\phi}/m_q^2}{q^2-m_q^2}\right] \mathcal{F}^2\left(q^2,m_q^2\right),$$

$$\mathcal{M}^{(a)}_{B^+\to D^{*+}X_0} = i^3 \int \frac{d^4q}{(2\pi)^4}\Big[\mathcal{A}^{B\to D_{s0}\bar{D}^*}_{\nu}(p_1,p_2)\Big] \times\Big[ig_{D_0D^*V}g_{\delta\beta}\epsilon^{\delta}(p_3)\Big]\Big[ig_{X_0}g_{\rho\phi}(p_4)\Big] \times\left[\frac{1}{p_1^2-m_1^2}\right]\left[\frac{-g^{\nu\rho}+p_2^{\nu}p_2^{\rho}/m_2^2}{p_2^2-m_2^2}\right] \times\left[\frac{-g^{\beta\phi}+q^{\beta}q^{\phi}/m_q^2}{q^2-m_q^2}\right]\mathcal{F}^2\left(q^2,m_q^2\right),$$

$$\mathcal{M}^{(b)}_{B^+\to D^{*+}X_0} = i^3 \int \frac{d^4q}{(2\pi)^4}\Big[\mathcal{A}^{B\to D_{s1}\bar{D}^*}_{\mu\nu}(p_1,p_2)\Big] \times\Big[ig_{D_1D^*V}\varepsilon_{\delta\beta\alpha\beta_2}(p_1+p_3)^{\beta_2}\epsilon^{\delta}(p_3)\Big]\Big[ig_{X_0}g_{\rho\phi}\Big] \times\left[\frac{-g^{\mu\alpha}+p_1^{\mu}p_1^{\alpha}/m_1^2}{p_1^2-m_1^2}\right]\left[\frac{-g^{\nu\rho}+p_2^{\nu}p_2^{\rho}/m_2^2}{p_2^2-m_2^2}\right] \times\left[\frac{-g^{\beta\phi}+q^{\beta}q^{\phi}/m_q^2}{q^2-m_q^2}\right]\mathcal{F}^2\left(q^2,m_q^2\right),$$

$$\mathcal{M}^{(a)}_{B^+\to D^{*+}\tilde{X}_1} = i^3 \int \frac{d^4q}{(2\pi)^4}\Big[\mathcal{A}^{B\to D_{s0}\bar{D}^*}_{\nu}(p_1,p_2)\Big] \times\Big[ig_{D_0D^*V}g_{\delta\beta}\epsilon^{\delta}(p_3)\Big] \times\Big[-g_{\tilde{X}_1}\varepsilon_{\mu_1\tau\rho\phi}p_4^{\mu_1}\epsilon^{\tau}(p_4)\Big] \times\left[\frac{1}{p_1^2-m_1^2}\right]\left[\frac{-g^{\nu\rho}+p_2^{\nu}p_2^{\rho}/m_2^2}{p_2^2-m_2^2}\right] \times\left[\frac{-g^{\beta\phi}+q^{\beta}q^{\phi}/m_q^2}{q^2-m_q^2}\right]\mathcal{F}^2\left(q^2,m_q^2\right),$$

$$\mathcal{M}^{(b)}_{B^+\to D^{*+}\tilde{X}_1} = i^3 \int \frac{d^4q}{(2\pi)^4}\Big[\mathcal{A}^{B\to D_{s1}\bar{D}^*}_{\mu\nu}(p_1,p_2)\Big] \times\Big[ig_{D_1D^*V}\varepsilon_{\delta\beta\alpha\beta_2}(p_1+p_3)^{\beta_2}\epsilon^{\delta}(p_3)\Big] \times\Big[-g_{\tilde{X}_1}\varepsilon_{\mu_1\tau\rho\phi}p_4^{\mu_1}\epsilon^{\tau}(p_4)\Big]$$

$$\times\left[\frac{-g^{\mu\alpha}+p_1^{\mu}p_1^{\alpha}/m_1^2}{p_1^2-m_1^2}\right]\left[\frac{-g^{\nu\rho}+p_2^{\nu}p_2^{\rho}/m_2^2}{p_2^2-m_2^2}\right]$$
$$\times\left[\frac{-g^{\beta\phi}+q^{\beta}q^{\phi}/m_q^2}{q^2-m_q^2}\right]\mathcal{F}^2\left(q^2,m_q^2\right),$$
$$\mathcal{M}^{(a)}_{B^+\to D^{*+}\tilde{X}_2}=i^3\int\frac{d^4q}{(2\pi)^4}\left[\mathcal{A}^{B\to D_{s0}\bar{D}^*}_{\nu}(p_1,p_2)\right]$$
$$\times\left[ig_{D_0D^*V}g_{\delta\beta}\epsilon^{\delta}(p_3)\right]\left[ig_{\tilde{X}_2}\epsilon_{\rho\phi}(p_4)\right]$$
$$\times\left[\frac{1}{p_1^2-m_1^2}\right]\left[\frac{-g^{\nu\rho}+p_2^{\nu}p_2^{\rho}/m_2^2}{p_2^2-m_2^2}\right]$$
$$\times\left[\frac{-g^{\beta\phi}+q^{\beta}q^{\phi}/m_q^2}{q^2-m_q^2}\right]\mathcal{F}^2\left(q^2,m_q^2\right),$$
$$\mathcal{M}^{(b)}_{B^+\to D^{*+}\tilde{X}_2}=i^3\int\frac{d^4q}{(2\pi)^4}\left[\mathcal{A}^{B\to D_{s1}\bar{D}^*}_{\mu\nu}(p_1,p_2)\right]$$
$$\times\left[ig_{D_1D^*V}\varepsilon_{\delta\beta\alpha\beta_2}(p_1+p_3)^{\beta_2}\epsilon^{\delta}(p_3)\right]$$
$$\times\left[ig_{\tilde{X}_2}\epsilon_{\rho\phi}(p_4)\right]\times\left[\frac{-g^{\mu\alpha}+p_1^{\mu}p_1^{\alpha}/m_1^2}{p_1^2-m_1^2}\right]$$
$$\times\left[\frac{-g^{\nu\rho}+p_2^{\nu}p_2^{\rho}/m_2^2}{p_2^2-m_2^2}\right]\left[\frac{-g^{\beta\phi}+q^{\beta}q^{\phi}/m_q^2}{q^2-m_q^2}\right]$$
$$\mathcal{F}^2\left(q^2,m_q^2\right). \tag{A 1}$$

References

1. S.L. Olsen, T. Skwarnicki, D. Zieminska, Rev. Mod. Phys. **90**(1), 015003 (2018). https://doi.org/10.1103/RevModPhys.90.015003. arXiv:1708.04012 [hep-ph]
2. N. Brambilla, S. Eidelman, C. Hanhart, A. Nefediev, C.P. Shen, C.E. Thomas, A. Vairo, C.Z. Yuan, Phys. Rep. **873**, 1–154 (2020). https://doi.org/10.1016/j.physrep.2020.05.001. arXiv:1907.07583 [hep-ex]
3. A. Ali, J.S. Lange, S. Stone, Prog. Part. Nucl. Phys. **97**, 123–198 (2017). https://doi.org/10.1016/j.ppnp.2017.08.003. arXiv:1706.00610 [hep-ph]
4. Y. Dong, A. Faessler, V.E. Lyubovitskij, Prog. Part. Nucl. Phys. **94**, 282–310 (2017). https://doi.org/10.1016/j.ppnp.2017.01.002
5. Y.R. Liu, H.X. Chen, W. Chen, X. Liu, S.L. Zhu, Prog. Part. Nucl. Phys. **107**, 237–320 (2019). https://doi.org/10.1016/j.ppnp.2019.04.003. arXiv:1903.11976 [hep-ph]
6. F.K. Guo, X.H. Liu, S. Sakai, Prog. Part. Nucl. Phys. **112**, 103757 (2020). https://doi.org/10.1016/j.ppnp.2020.103757. arXiv:1912.07030 [hep-ph]
7. X. Liu, Chin. Sci. Bull. **59**, 3815–3830 (2014). https://doi.org/10.1007/s11434-014-0407-2. arXiv:1312.7408 [hep-ph]
8. F.K. Guo, C. Hanhart, U.G. Meißner, Q. Wang, Q. Zhao, B.S. Zou, Rev. Mod. Phys. **90**(1), 015004 (2018). https://doi.org/10.1103/RevModPhys.90.015004. arXiv:1705.00141 [hep-ph]. [erratum: Rev. Mod. Phys. 94, 2, 029901 (2022)]
9. S.K. Choi et al. [Belle], Phys. Rev. Lett. **91**, 262001 (2003). https://doi.org/10.1103/PhysRevLett.91.262001. arXiv:hep-ex/0309032
10. M. Ablikim et al. [BESIII], Phys. Rev. Lett. **111**(24), 242001 (2013). https://doi.org/10.1103/PhysRevLett.111.242001. arXiv:1309.1896 [hep-ex]
11. M. Ablikim et al. [BESIII], Phys. Rev. Lett. **112**(13), 132001 (2014). https://doi.org/10.1103/PhysRevLett.112.132001. arXiv:1308.2760 [hep-ex]
12. R. Aaij et al. [LHCb], Phys. Rev. D **102**, 112003 (2020). https://doi.org/10.1103/PhysRevD.102.112003. arXiv:2009.00026 [hep-ex]
13. R. Aaij et al. [LHCb], Phys. Rev. Lett. **125**, 242001 (2020). https://doi.org/10.1103/PhysRevLett.125.242001. arXiv:2009.00025 [hep-ex]
14. T. Guo, J. Li, J. Zhao, L. He, Phys. Rev. D **105**(5), 054018 (2022). https://doi.org/10.1103/PhysRevD.105.054018. arXiv:2108.06222 [hep-ph]
15. J.R. Zhang, Phys. Rev. D **103**(5), 054019 (2021). https://doi.org/10.1103/PhysRevD.103.054019. arXiv:2008.07295 [hep-ph]
16. Z.G. Wang, Int. J. Mod. Phys. A **35**(30), 2050187 (2020). https://doi.org/10.1142/S0217751X20501870. arXiv:2008.07833 [hep-ph]
17. X.G. He, W. Wang, R. Zhu, Eur. Phys. J. C **80**(11), 1026 (2020). https://doi.org/10.1140/epjc/s10052-020-08597-1. arXiv:2008.07145 [hep-ph]
18. G.J. Wang, L. Meng, L.Y. Xiao, M. Oka, S.L. Zhu, Eur. Phys. J. C **81**(2), 188 (2021). https://doi.org/10.1140/epjc/s10052-021-08978-0. arXiv:2010.09395 [hep-ph]
19. Q.F. Lü, D.Y. Chen, Y.B. Dong, Phys. Rev. D **102**(7), 074021 (2020). https://doi.org/10.1103/PhysRevD.102.074021. arXiv:2008.07340 [hep-ph]
20. S.S. Agaev, K. Azizi, H. Sundu, Phys. Rev. D **106**(1), 014019 (2022). https://doi.org/10.1103/PhysRevD.106.014019. arXiv:2204.08498 [hep-ph]
21. R. Molina, T. Branz, E. Oset, Phys. Rev. D **82**, 014010 (2010). https://doi.org/10.1103/PhysRevD.82.014010. arXiv:1005.0335 [hep-ph]
22. H.W. Ke, Y.F. Shi, X.H. Liu, X.Q. Li, Phys. Rev. D **106**(11), 114032 (2022). https://doi.org/10.1103/PhysRevD.106.114032. arXiv:2210.06215 [hep-ph]
23. S.Y. Kong, J.T. Zhu, D. Song, J. He, Phys. Rev. D **104**(9), 094012 (2021). https://doi.org/10.1103/PhysRevD.104.094012. arXiv:2106.07272 [hep-ph]
24. B. Wang, S.L. Zhu, Eur. Phys. J. C **82**(5), 419 (2022). https://doi.org/10.1140/epjc/s10052-022-10396-9. arXiv:2107.09275 [hep-ph]
25. H.X. Chen, Phys. Rev. D **105**(9), 094003 (2022). https://doi.org/10.1103/PhysRevD.105.094003. arXiv:2103.08586 [hep-ph]
26. S.S. Agaev, K. Azizi, H. Sundu, J. Phys. G **48**(8), 085012 (2021). https://doi.org/10.1088/1361-6471/ac0b31. arXiv:2008.13027 [hep-ph]
27. H.X. Chen, W. Chen, R.R. Dong, N. Su, Chin. Phys. Lett. **37**(10), 101201 (2020). https://doi.org/10.1088/0256-307X/37/10/101201. arXiv:2008.07516 [hep-ph]
28. H. Mutuk, J. Phys. G **48**(5), 055007 (2021). https://doi.org/10.1088/1361-6471/abeb7f. arXiv:2009.02492 [hep-ph]
29. M.Z. Liu, J.J. Xie, L.S. Geng, Phys. Rev. D **102**(9), 091502 (2020). https://doi.org/10.1103/PhysRevD.102.091502. arXiv:2008.07389 [hep-ph]
30. C.J. Xiao, D.Y. Chen, Y.B. Dong, G.W. Meng, Phys. Rev. D **103**(3), 034004 (2021). https://doi.org/10.1103/PhysRevD.103.034004. arXiv:2009.14538 [hep-ph]
31. Y. Huang, J.X. Lu, J.J. Xie, L.S. Geng, Eur. Phys. J. C **80**(10), 973 (2020). https://doi.org/10.1140/epjc/s10052-020-08516-4. arXiv:2008.07959 [hep-ph]
32. E.S. Swanson, Nucl. Part. Phys. Proc. **312–317**, 130–134 (2021). https://doi.org/10.1016/j.nuclphysbps.2021.05.033

33. T.J. Burns, E.S. Swanson, Phys. Rev. D **103**(1), 014004 (2021). https://doi.org/10.1103/PhysRevD.103.014004. arXiv:2009.05352 [hep-ph]
34. Q.Y. Lin, X.Y. Wang, Eur. Phys. J. C **82**(11), 1017 (2022). https://doi.org/10.1140/epjc/s10052-022-10995-6. arXiv:2209.06062 [hep-ph]
35. Y.K. Hsiao, Y. Yu, Phys. Rev. D **104**(3), 034008 (2021). https://doi.org/10.1103/PhysRevD.104.034008. arXiv:2104.01296 [hep-ph]
36. P.A. Zyla et al. [Particle Data Group], PTEP **2020**(8), 083C01 (2020). https://doi.org/10.1093/ptep/ptaa104
37. M.W. Hu, X.Y. Lao, P. Ling, Q. Wang, Chin. Phys. C **45**(2), 021003 (2021). https://doi.org/10.1088/1674-1137/abcfaa. arXiv:2008.06894 [hep-ph]
38. J. He, D.Y. Chen, Chin. Phys. C **45**(6), 063102 (2021). https://doi.org/10.1088/1674-1137/abeda8. arXiv:2008.07782 [hep-ph]
39. R. Molina, E. Oset, Phys. Lett. B **811**, 135870 (2020). https://doi.org/10.1016/j.physletb.2020.135870. arXiv:2008.11171 [hep-ph]. [erratum: Phys. Lett. B 837, 137645 (2023)]
40. L.R. Dai, R. Molina, E. Oset, Phys. Rev. D **105**(9), 096022 (2022). https://doi.org/10.1103/PhysRevD.105.096022. arXiv:2202.11973 [hep-ph]
41. M. Bayar, E. Oset, Phys. Lett. B **833**, 137364 (2022). https://doi.org/10.1016/j.physletb.2022.137364. arXiv:2207.02577 [hep-ph]
42. Y.K. Chen, J.J. Han, Q.F. Lü, J.P. Wang, F.S. Yu, Eur. Phys. J. C **81**(1), 71 (2021). https://doi.org/10.1140/epjc/s10052-021-08857-8. arXiv:2009.01182 [hep-ph]
43. H.Y. Cheng, C.K. Chua, C.W. Hwang, Phys. Rev. D **69**, 074025 (2004). https://doi.org/10.1103/PhysRevD.69.074025. arXiv:hep-ph/0310359
44. N.R. Soni, A. Issadykov, A.N. Gadaria, Z. Tyulemissov, J.J. Patel, J.N. Pandya, Eur. Phys. J. Plus **138**(2), 163 (2023). https://doi.org/10.1140/epjp/s13360-023-03779-8. arXiv:2110.12740 [hep-ph]
45. M. Bauer, B. Stech, M. Wirbel, Z. Phys. C **34**, 103 (1987). https://doi.org/10.1007/BF01561122
46. A. Ali, G. Kramer, C.D. Lu, Phys. Rev. D **58**, 094009 (1998). https://doi.org/10.1103/PhysRevD.58.094009. arXiv:hep-ph/9804363
47. M.A. Ivanov, J.G. Korner, P. Santorelli, Phys. Rev. D **73**, 054024 (2006). https://doi.org/10.1103/PhysRevD.73.054024. arXiv:hep-ph/0602050
48. D.S. Hwang, D.W. Kim, Phys. Lett. B **606**, 116–122 (2005). https://doi.org/10.1016/j.physletb.2004.11.035. arXiv:hep-ph/0410301
49. R. Casalbuoni, A. Deandrea, N. Di Bartolomeo, R. Gatto, F. Feruglio, G. Nardulli, Phys. Rep. **281**, 145–238 (1997). https://doi.org/10.1016/S0370-1573(96)00027-0. arXiv:hep-ph/9605342
50. R. Casalbuoni, A. Deandrea, N. Di Bartolomeo, R. Gatto, F. Feruglio, G. Nardulli, Phys. Lett. B **292**, 371–376 (1992). https://doi.org/10.1016/0370-2693(92)91189-G. arXiv:hep-ph/9209248
51. R. Casalbuoni, A. Deandrea, N. Di Bartolomeo, R. Gatto, F. Feruglio, G. Nardulli, Phys. Lett. B **299**, 139–150 (1993). https://doi.org/10.1016/0370-2693(93)90895-O. arXiv:hep-ph/9211248
52. H.Y. Cheng, C.K. Chua, A. Soni, Phys. Rev. D **71**, 014030 (2005). https://doi.org/10.1103/PhysRevD.71.014030. arXiv:hep-ph/0409317
53. D. Gamermann, J. Nieves, E. Oset, E. Ruiz Arriola, Phys. Rev. D **81**, 014029 (2010). https://doi.org/10.1103/PhysRevD.81.014029. arXiv:0911.4407 [hep-ph]
54. M. Bayar, R. Molina, E. Oset, M.Z. Liu, L.S. Geng, arXiv:2312.12004 [hep-ph]
55. R. Mertig, M. Bohm, A. Denner, Comput. Phys. Commun. **64**, 345–359 (1991). https://doi.org/10.1016/0010-4655(91)90130-D
56. T. Hahn, M. Perez-Victoria, Comput. Phys. Commun. **118**, 153–165 (1999). https://doi.org/10.1016/S0010-4655(98)00173-8. arXiv:hep-ph/9807565
57. G.J. Ding, Phys. Rev. D **79**, 014001 (2009). https://doi.org/10.1103/PhysRevD.79.014001. arXiv:0809.4818 [hep-ph]
58. R.C. Verma, J. Phys. G **39**, 025005 (2012). https://doi.org/10.1088/0954-3899/39/2/025005. arXiv:1103.2973 [hep-ph]